

DEVELOPMENT AND EVALUATION OF A HUMAN LOWER EXTREMITY MODEL

Yuichi Kitagawa

Chinmoy Pal

NISSAN MOTOR CO., LTD.

Japan

Paper Number: 282

ABSTRACT

A finite element model of the human lower extremity has been developed in this study to simulate lower extremity behavior in frontal car crashes. Precise geometry of the human lower extremity and material properties of the hard and soft tissues were introduced to the model. The performance of the model was evaluated by comparing with dynamic loading test data using post mortem human subjects (PMHS). The comparison proved its ability to estimate dynamic responses of the human lower extremity. A study was conducted using the model to investigate possible factors of loading to the ankle and tibia. Force and moment was calculated with different time history profiles of footwell intrusion and pelvis motion. The results suggested that timing of maximum intrusion was important as well as its magnitude. It was also found that loading to the tibia could be affected not only by intrusion but also by pelvis motion. Although footwell deformation has been measured in car crash tests, it is suggested to use force and moment measured on the dummy leg for injury assessment.

INTRODUCTION

A numbers of studies has been done to understand injury mechanisms to the lower extremity. Morgan et al. (1991) characterized loading patterns of the ankle and foot based on the NASS data. They found that contact with foot controls accounted for 43 percent of the occupants with ankle injuries followed by contact with the floor accounting for 24 percent. It was also pointed out that another 12 percent was related to the

knee entrapment. Taylor et al. (1997) analyzed the CCIS database adopting the hypothesis proposed by Morgan. They concluded that intrusion was considered to be responsible for severe lower extremity injuries. The relationship between crash severity and intrusion was, however, not determined by the accident data. Another study on the CCIS by Thomas et al. (1995) concluded that intrusion was still a major cause of lower extremity injury despite the fact that it was not necessarily a proxy variable for delta-V. A different approach has been made by Crandall et al. (1996) by conducting a series of sled tests with toe pan intrusion using PMHS specimens. Among different magnitude of intrusion, there was only one injured case out of twelve specimens under the largest intrusion. They also conducted a simulation study using the ATB program and pointed out that tibia force could be greatly affected by the knee entrapment. Further studies are, therefore, necessary to understand injury mechanisms more in detail.

In cadaver tests, load cells are used to measure force and moment in the specimen and accelerometers are mounted to detect kinematics of the joints. Although the test result reveals injury outcome under a given loading condition, it is sometimes difficult to precisely explain injury mechanisms due to variety in cadaver property and scattering in test data. Repeatability is one of the benefits of using human models. Once a model is developed and validated, it can be used unlimited times and its response is always identical. The other benefit is visualization. Visualized stress and strain can help us understand injury

mechanisms. Finite element models of human body parts such as head, neck, thorax, spine, pelvis, upper and lower extremities have been developed. Mesh is generated based on human body geometry database and material properties are generally taken from literatures. When joints are included, ligaments and tendons are modeled as well as bones. Muscles are also taken into account when their passive or active effects are not negligible.

The goal of this research is to investigate possible factors related to lower extremity injuries in frontal crashes, focusing on fractures in tarsal (ankle) bones and tibia. These injuries are thought to be caused by footwell intrusion in high-speed crashes. First, a finite element model of the human lower extremity was developed and evaluated. The distal part of the model is based on the ankle and foot model developed by Beaugonin et al. The model was validated against ankle rotations in inversion, eversion and dorsiflexion tests conducted at Wayne State University (1996, 1997). The model was used by the authors to study ankle injury mechanisms with muscular tension (1998). A stress concentration was found in the distal tibia corresponding to the fractured area in cadaver tests. The authors have added some ligaments and tendons to simulate foot deformation under high compressive force. Skin and fat layers were also modeled to reproduce realistic interaction with impactors. The revised model showed a good match with cadaver responses in both static and dynamic loading tests (2000). In this study, the model was extended up to the proximal femur in order to simulate kinematics of the whole lower extremity of an occupant. Validation was made against human cadaver data obtained in impactor tests conducted at UVA (1997). Then a simplified vehicular interior model was created so that it can reproduce footwell intrusion and pelvis motion in a frontal crash. A parametric study was performed by changing time history profiles of footwell intrusion and pelvis motion. Tibial force and moment were calculated to estimate

loading level to the lower extremity. This paper introduces the model description and its validation, and discusses possible factors related to lower extremity injuries.

MODEL DESCRIPTION

Figure 1 shows an entire view of the lower extremity model. The distal part of the model derived from the ankle and foot model developed by the authors while the mesh of the knee area was taken from the H-Dummy knee model which was originally developed by Choi et al (1998). Although this study does not focus on injuries in these areas, the model was expected to be useful to simulate kinematics of the whole lower extremity. The model essentially corresponds to the skeletal system of an average human right lower extremity as developed by Beaugonin et al. The geometry of bones from the foot up to the femur were accurately depicted in the model. A cortical part was modeled by shell elements and a trabecular part was modeled by solid elements. Some principal bones that were likely to be involved in ankle and tibia injuries, such as tarsal bones, were modeled by deformable elements. Fracture cannot be simulated in the model because linearly elastic material was assumed for the deformable elements. Shell elements were used for the phalanges as their deformation was negligible in this study. Skin and fat layers were generated surrounding the bony model except small areas surrounding the

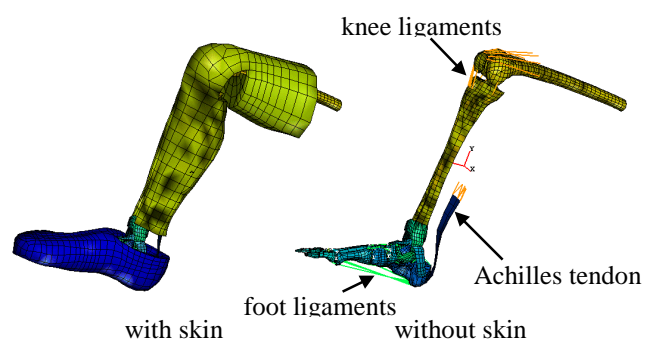


Figure 1. Lower Extremity Model.

ankle joint. The anterior part of the knee joint was covered with shell elements in order to simulate a contact with an instrument panel. The total number of nodes in this model was 9449 with 4053 shells and 5340 solid elements. The element size tends to be small especially in joints to represent precise geometry of the articular surfaces. The meshes were carefully checked to stabilize the time integration scheme and to reduce the computational time. The time step was $0.8e-5$ msec in the authors' previous study. It was increased to $0.2e-4$ msec in the revised model. As more than half of computational power was spent on calculating internal forces in this model, the total reduction in CPU time was around 50%. The material properties for the bony parts and skin/fat layers were taken from the authors' model while those for the knee ligaments were taken from the H-Dummy knee model.

MODEL VALIDATION

PMHS Test

A series of impactor tests was conducted at the University of Virginia, Auto Safety Lab. Human lower extremity specimens were obtained from medical cadavers in accordance with ethical guidelines and research protocol. All specimens were allowed to sectioned above the knee at mid-femur to preserve the functional anatomy of the knee joint and leg musculature. Their properties are listed in Table 1. Specimens were instrumented with an implanted tibia load cell to measure the tibial forces and moments. Figure 2 shows a schematic of the test apparatus. The specimen was mounted in a position simulating driver geometry. A rigid bar was attached to the femur to reproduce the original hip to knee length of the

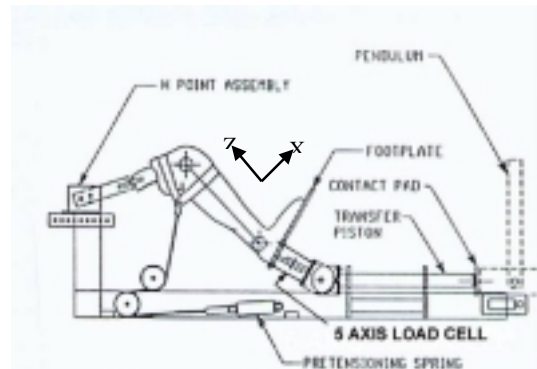


Figure 2. PMHS Test Apparatus.

specimen. The femur was positioned and rotated to correct for the natural valgus angle at the knee such that the long axis of the tibia would be aligned with the direction of impact when the foot was placed on the footplate. A 9.5 mm thick piece of foam padding was placed between the foot and the footplate to damp out oscillation. The effect of occupant bracing was simulated externally with a harness placed over the knee which was attached to a spring via a pulley. Immediately before impact, the knee harness was tightened until the axial load in the specimen reached half of the specimen's body weight. Impacting energy was generated by a rigid pendulum which was given initial potential energy at the beginning. All electric data were sampled at 10,000 Hz using a DSP TRAQ-P data analysis system and digitally filtered to SAE J211 channel class 180. Video data were taken from each test using a high-speed (1000 fps) Kodak RO color imager. Load cell data were debiased using offsets recorded in an unloaded state immediately prior to initial positioning. All output files have been truncated to include only data between -10 and 150 msec.

Table 1. Cadaver Properties

Test	Specimen	Age	L/R	Sex	Height	Mass	Foot angle	Tibia angle	Femur angle
36a	98-FM-4-R	81	R	M	173 cm	63.6 kg	75 deg.	15 deg.	30 deg.
36c	98-FM-4-L	81	L	M	173 cm	63.6 kg	75 deg.	17 deg.	30 deg.
37b	98-FM-94-L	65	L	M	NA	99.1 kg	75 deg.	16 deg.	30 deg.
37c	97-EF-79-L	54	L	F	152 cm	71.8 kg	75 deg.	17 deg.	25 deg.

Test Results

Only uninjured specimens were selected for model validation because the simulation model is basically elastic. The average impact speed was around 6 m/s. There were four cases where the specimen did not sustain any fractures during dynamic loading. The tibial axial force(1) and the tibial sagittal moment(2) were plotted in Figure 3. The effect of preloading can be seen as an initial positive offset in the tibial force. There was just a single peak in the force curve which was generated after impacted by the pendulum. As generally seen in most cadaver tests, the response curves were slightly different among individuals. Difference in preloading also affected the load cell readings. The maximum peak in the tibial force varied from 7 to 10 kN. A corridor was created for model validation based on the data. For the moment result, no common trend was found in the time history curves. A possible explanation is that the moment was greatly affected by the specimen length and its posture. Although the posture was carefully adjusted so that the joint angles reached specified values, it slightly changed when preloaded. No explanation was found for specimen 37b. Since this is the only case showing large positive moment, it should be treated carefully in the model validation.

Simulation Model

An equivalent condition to the PMHS test was carefully simulated in the model. The initial angles in the ankle and knee joints were adjusted to the average values measured in the tests. A rigid bar was defined at the proximal end of the femur and its end was fixed to the inertial space only allowing the sagittal rotation. A footplate model was generated and located just beneath the foot. The 9.5 mm of foam padding was modeled by a single layer of solid elements. Its material property was obtained by a dynamic compression test performed on a sample piece. The knee straps were modeled by membrane elements contacting the skin

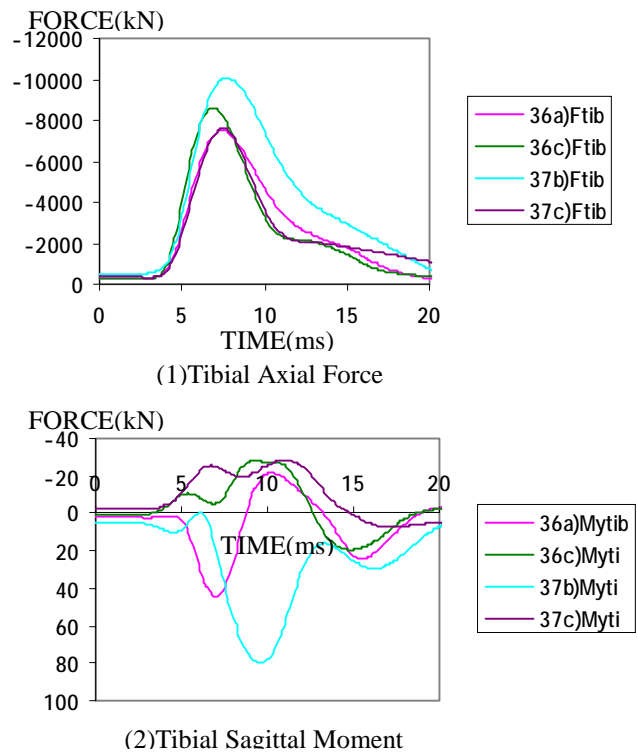


Figure 3. PMHS Test Results.

surfaces. A half body weight of pretensioning was applied to the spring element which was connected to the end of the knee straps. The pretensioning force was gradually increased using a cosine curve not to generate unnecessary oscillation. Dynamic loading was simulated by moving the footplate. Its motion was defined by a time history curve which was obtained by double integrating the footplate acceleration measured in the test. The footplate was only allowed to move in the horizontal direction. Contact interaction was specified between the foot and the footplate. A section and a local coordinate frame were defined in the tibia in order to calculate force and moment during impact. The simulation was performed by an explicit integration procedure using PAM-CRASH. The calculation was terminated when the time reached 20 msec after impact.

Simulation Results

The calculated force and moment were compared with the test data. Figure 4 shows the

comparisons of time history curves between the simulation results and test results. In each graph, the simulation result was plotted in a black curve while the gray area indicated a corridor of the cadaver response. The kinetic energy of the pendulum was almost diminished at 20 ms after impact. The calculated tibial axial force(1) showed a similar profile to the cadaver test data. The only difference was that the calculated force did not decrease immediately after the maximum peak. The tibial sagittal moment(2) was found in the corridor except for its end. If the data from specimen 37b was removed in Figure 3, the result matches well with the other three cases. Figure 5 compares the postures of the lower extremity at 20 ms after impact between the simulation result and the test result. The gross motion was similar to each other. Summarizing the comparisons, the developed lower extremity model showed an acceptable match with cadaver test data.

PARAMETRIC STUDY

Loading Model

A parametric study was conducted to investigate relationship between boundary conditions and resultant loading to the lower extremity. Intrusion was taken as a parameter, since it has been suggested as a major cause of ankle and tibia injuries. Forward motion of the pelvis was taken as another parameter because it could affect knee entrapping condition. A loading model was created simulating typical geometry of the front seat area of a vehicle compartment. Figure 6 shows an entire view of the model. A footwell was modeled as a bent plate which consisted of a horizontal part supporting the heel and a steep part representing a toepan. A rigid body system was defined for the footwell and its control point was located at lower side of the model. By rotating the footwell system around the control point, realistic intrusion was generated so that the top edge moved further than the bottom edge. Pelvis motion was simulated by moving the hip point forward. Another rigid body system was defined

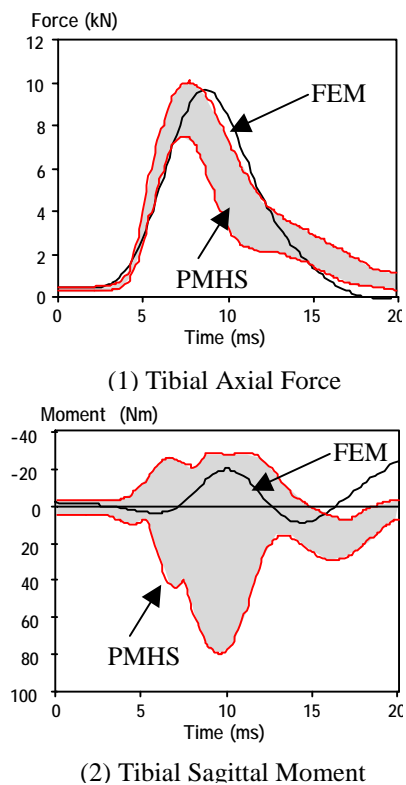
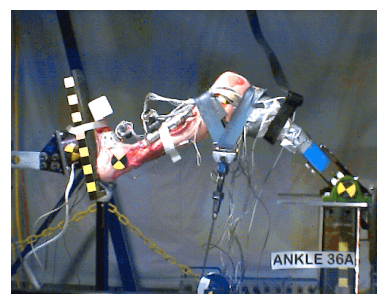
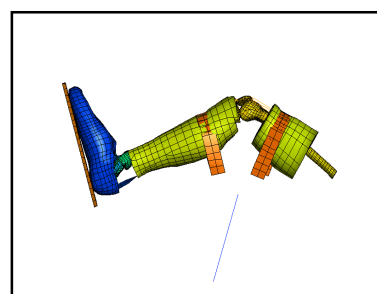


Figure 4. Comparison of Force/Moment.



PMHS Test



FEM Model

Figure 5. Comparison of Gross Motion.

connecting the hip point to the proximal end of femur. Rotation of the hip point was allowed assuming that muscular effects were negligible on the femur behavior. A flat plate, ahead of the knee, represented an instrument panel in a vehicle compartment. Its surrounding edge was fixed to the inertial space and the material was assumed so that it allowed a few inches of deformation when impacted by the knee. The initial posture of the lower extremity and location of panels were defined with reference to a small passenger vehicle. Acceleration was given to the entire system to simulate a decelerating compartment in a frontal crash. The acceleration data was obtained from a car crash test. Table 2 is the simulation matrix and Figure 7 shows function curves that were used to control the footwell intrusion and the pelvis motion. Case 1 was taken as the base line. The maximum magnitude of the functions was reduced by half in Case 2 and 3, while the timing of the maximum peak was shifted in Case 4 and 5.

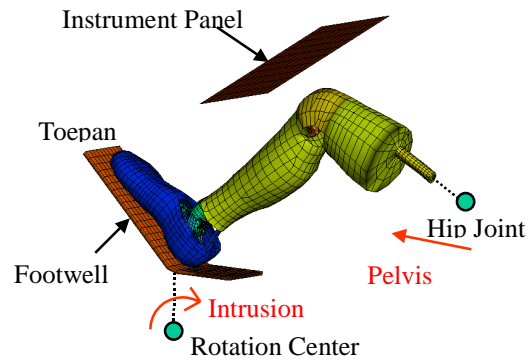


Figure 6. Loading Model.

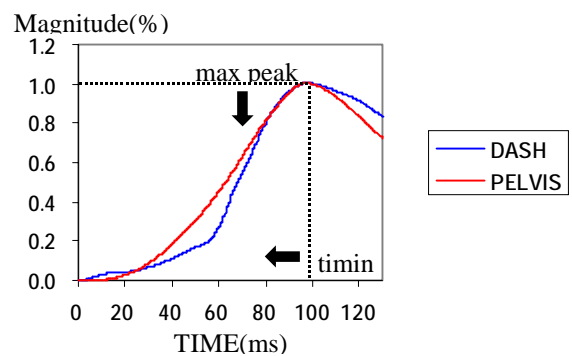


Figure 7. Loading Functions.

Results and Discussion

Calculated tibia and femur forces were plotted in Figure 8, taken from the result of the first case. A few peaks can be noticed in the tibia force while the femur force has only one prominent peak. The first one rose when the foot was impacted by the toe pan. The footwell intrusion merely generated the second peak. The foot was pushed rearward by the footwell while the knee was moving forward. It can be explained that the combined motions resulted in compression of the tibia. The later peaks appeared after the knee contacted the instrument panel. It can be known by the maximum peak of the femur force. The femur force level was not significant under the given condition but

its timing should be monitored. The sagittal moment was also calculated in the tibia. It was plotted in Figure 9 with distance change between the foot and the proximal femur. It is clear that the moment was generated as the two points became closer.

Figure 10 compares the maximum peaks in the tibia force from Case 1 to Case 3. The peak was mitigated in the second case where the maximum level of intrusion was reduced by half. The peak slightly increased in the third case where the pelvis motion was restrained. These results support the interpretation that intrusion could be a major factor of ankle and tibia injuries. Another explanation is necessary, however, for

Table 2. Simulation Matrix

Case	Footwell Intrusion		Pelvis Motion	
	Max Magnitude	Max Time	Max Displ.	Max Time
1	168 mm	98 ms	160 mm	98 ms
2	x 0.5	x 1.0	x 1.0	x 1.0
3	x 1.0	x 1.0	x 0.5	x 1.0
4	x 1.0	x 0.8	x 1.0	x 1.0
5	x 1.0	x 1.0	x 1.0	x 0.65

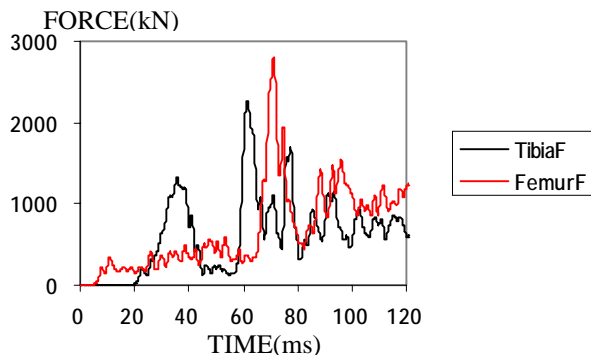


Figure 8. Forces in Tibia and Fibula.

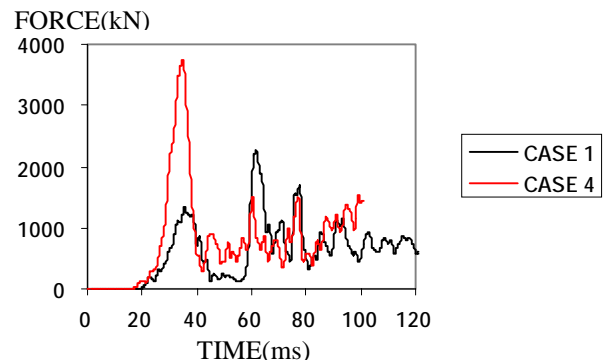


Figure 11. Effect of Intruding Timing.

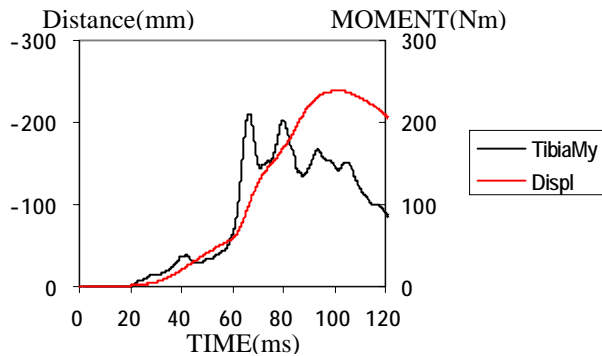


Figure 9. Tibia Moment and Joints Distance.

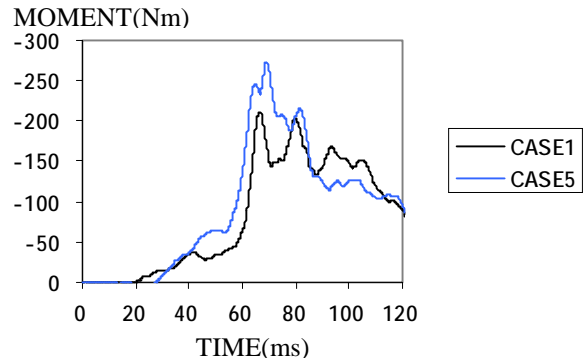


Figure 12. Effect of Timing of Pelvis Motion.

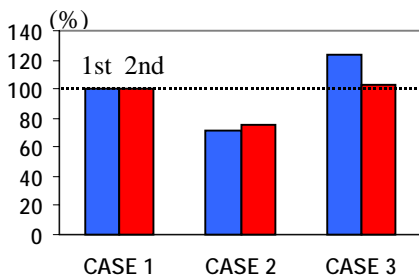


Figure 10. Effect of Intrusion Magnitude on Tibia Force Peaks (Max and 2nd).

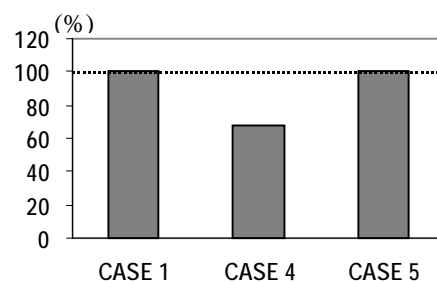


Figure 13. Comparison of Distance between Ankle and Hip Joints (max shortening).

the result of Case 4 in Figure 11. Higher peak was observed in the tibia force compared with that in the first case where the magnitude of intrusion was exactly the same. The only difference between them was the timing of peak intrusion. The result indicates that timing can greatly affect resultant force. It should be also noted that the first one was the maximum among the peaks in the tibia force. It means that loading to the tibia concentrated during that period. The other finding was found in the moment curve shown in Figure 12, where the pelvis motion was hastened as Case 5. As the knee contacted the instrument panel earlier, the tibia

was compressed between the footwell and the instrument panel. Large moment was generated in the tibia, while no significant increase was found in the axial force owing to soft material of the instrument panel. The result suggests that combined motions of the foot and the pelvis increased the tibia moment. It can be explained by the horizontal distance between the foot and the pelvis, plotted in Figure 13. Summarizing the comparisons including the last two cases, it can be concluded that the magnitude of intrusion is not the only factor which determines loading to the lower extremity. Time history profile of intrusion and its

relation with pelvis motion should be also considered. Since an experimental technique is not established for dynamic measurement of footwell intrusion, it is difficult at present to accurately evaluate a loading level to the lower extremity in a car crash test. It is considered that the evaluation should be made on the dummy leg, which has a good biofidelity such as the Thor-lx, rather than on a vehicle body.

CONCLUSION

A finite element model of the human lower extremity was developed in this study. Precise geometry of bones, ligaments, tendons, skin and fat layers were carefully duplicated in the model. Material properties of hard and soft tissues were defined with reference with literatures. The performance of the model was evaluated by comparing with cadaver responses obtained through a series of sled tests conducted at the University of Virginia. It was confirmed that the calculated force was reliable to estimate loading condition to the tibia.

A parametric study was conducted using the model to investigate possible factors of loading to the ankle and tibia. A simplified vehicular interior model was generated which reproduced footwell intrusion and pelvis motion. Intrusion was still thought to be a major factor of ankle and tibia injuries, but the timing of maximum intrusion was also important not only its magnitude. The results also suggested that both footwell intrusion and pelvis motion should be monitored when analyzing the lower extremity behavior. For lower extremity injury assessment in a car crash test, evaluating force and moment on the dummy leg is more rational rather than measuring footwell deformation.

ACKNOWLEDGMENTS

The original finite element model of the human ankle/foot was developed by Beaugonin et al., ESI France. The validation of the ankle and foot model

was performed using the cadaver test data by Wanye State University. The H-Dummy knee model was developed by Choi et al., Hong-ik University, Korea. Technical supports were provided by Nihon ESI, Japan. The PMHS tests were conducted at University of Virginia.

REFERENCES

1. Beaugonin, M., Haug, E., Cesari, D. (1996); A Numerical Model of the Human Ankle/Foot Under Impact Loading in Iversion and Eversion, Proc. 40th Stapp Car Crash Conference, SAE 962428.
2. Beaugonin, M., Haug, E., Munck, G., Cesari, D. (1997); Improvement of Numerical Ankle/Foot Model: Modeling of Deformable Bone, Proc. 41th Stapp Car Crash Conference, SAE 973331.
3. Crandall, J., Bass, C., Klopp, G., Pilkey, W. (1996); Sled Tests With Toepan Intrusion Using Post-Mortem Human Surrogates and The Hybrid III Dummy, Proc. 1996 IRCOBI Conference, 339-352.
4. H-Dummy Version 1.6 User's Manual, Engineering Systems International, 1998.
5. Kitagawa, Y., Ichikawa, H., King, A., Begeman, C. (1998); A Severe Ankle and Foot Injury in Frontal Crashes and Its Mechanism, Proc. 42th Stapp Car Crash Conference, SAE 983145.
6. Kitagawa, Y., Ichikawa, H., King, A., Begeman, C. (2000); Finite Element Simulation of Ankle/Foot Injury in Frontal Crashes, SAE Paper 2000-01-0156.
7. Klopp, G., Crandall, J., Hall, G., Pilkey, W., Hurwitz, S., Kupp, S. (1997); Mechanisms of Injury and Injury Criteria for the Human Foot and Ankle in Dynamic Axial Impacts to the Foot, Proc. 1997 IRCOBI Conference, 73-86.

8. Morgan, R., Eppinger, R. (1991); Ankle Joint Injury Mechanism for Adults in Frontal Automotive Impact, Proc. 35th Stapp Car Crash Conference, SAE 912902.

9. Taylor A., Morris, A. P., Thomas, P., Wallace, A. (1997); Mechanisms of Lower Extremity Injuries to Front Seat Car Occupants – An In-Depth Accident Analysis, Proc. 1997 IRCOBI Conference, 53-72.

10. Thomas, P., Charles, J., Fay, P. (1995); Lower Limb Injuries – The Effect of Intrusion, Crash Severity and the Pedals on Injury Risk and Injury Type in Frontal Collisions, Proc. 39th Stapp Car Crash Conference, SAE 952728.